A facile method for promoting activities of vanadium–schiffbase complex anchored on organically modified MCM-41 in epoxidation reaction

K.M. Parida[*], Sudarshan Singha, P.C. Sahoo

Colloids and Materials Chemistry Department, Institute of Minerals & Materials Technology, Bhubaneswar-751013, Orissa, India

ABSTRACT

An organic–inorganic hybrid heterogeneous catalyst (V-MCM-41) was synthesized by anchoring vanadium–schiffbase complex on chloropropyl modified mesoporous silica (CP-MCM-41). Characterization of the functionalized ordered two-dimensional mesoporous material by powder X-ray diffraction (XRD), N_2 adsorption–desorption, CP-MAS NMR spectroscopy (^{13}C and ^{29}Si), Fourier transform infrared spectroscopy (FT-IR), diffuse-reflectance UV–vis spectroscopy, demonstrate the successful grafting of vanadium complex into the functionalized mesoporous silica. It is also observed that the mesostructure has not been destroyed in multistep synthetic procedure. We have performed the epoxidation reaction of various olefins using V-MCM-41 as the catalyst, hydrogen peroxide as the oxidant and sodium bicarbonate as the co-catalyst in acetonitrile solvent. The co-catalyst enhances the rate of reaction by many folds. The reaction requires minimum amount of H_2O_2, short time period and most importantly occurs at room temperature. The heterogeneous catalyst can be recovered easily and reused many times without significant loss in catalytic activity and selectivity.

© 2010 Elsevier B.V. All rights reserved.

1. Introduction

The discovery of efficient method for catalytic epoxidation is an important goal in synthetic chemistry as there is a growing interest in using epoxide as building block in organic synthesis. Developing systems that achieve high selectivity using environmental friendly conditions and inexpensive terminal oxidants remain as an important challenge [1,2]. In this context, H_2O_2 is probably the best ecological sustainable green terminal oxidant after dioxygen as water is the only byproduct. In certain circumstances, it is better than O_2 in so far as O_2–organic mixtures sometimes spontaneously ignite. In actual epoxidation process, alkyl hydroperoxide is used as oxidant. Since alkyl hydroperoxide is traditionally obtained by the reaction of H_2O_2 and aliphatic acid or acid derivatives, the epoxidation reaction in alkyl hydroperoxide generates a significant amount of waste and co-products [3,4].

The use of transition metal complexes as catalyst has been receiving increasing attention during past two decades due to many reasons: (1) the requirement for the functionalization of lower alkenes formed as byproducts in the manufacture of gasoline, (2) the need for partial selective oxidation and (3) the preparation of compounds with a specific spatial structure. The transition metal complexes seem to fulfill some of these requirements. Vanadium pentoxide was probably one of the first transition metal com-

plex used in epoxidation taking tert-butylhydroperoxide as oxidant [5]. Schiffbase complex bearing salen ligand represents one of the effective catalytic systems for the epoxidation of olefins. Recently vanadyl acetylacetonate grafting on to mesoporous silica used for the epoxidation of geraniols has been reported by Jarris et al. [6]. Transition metal schiffbase complexes (e.g., $M = Mn^{2+}$, Ni^{2+}, Fe^{3+}, Co^{2+}, and Cu^{2+}) chemically anchored on Y zeolite (partially modified by n-octadecyltrichlorosilane) have been applied to the epoxidation of 1-octene [7]. However, these catalysts have very low reactivity (conversion <3% after 24 h at 100 °C) despite high selectivity to epoxide (96%). Busch et al. reported olefin epoxidation by the hydrogen peroxide adduct of a novel non-heme manganese (IV) complex, where they demonstrate the oxygen transfer by multiple mechanisms [8]. The asymmetric epoxidation of olefins catalyzed by the manganese–salen complexes developed by Jacobsen et al. provides an easy approach to unfunctionalized epoxides [9].

Complex encapsulation and methodologies involving grafting and tethering procedures have been shown several advantages over method based on non-covalent interaction such as electrostatic, $\pi-\pi^*$, hydrophobic/hydrophilic interactions and hydrogen bonds [10]. The heterogenization of homogeneous catalyst has gained considerable interest over the last few decades; the most attractive advantage is the easy separation of the product from the catalyst without tedious experimental work-up. Mesoporous silica is a kind of ideal support which possess high surface area and ordered mesoporous channels [11,12]. This will be beneficial to the enhancement of loading amounts and dispersion of catalytic active sites. The preparation of organic–inorganic hybrid materi-

* Corresponding author. Tel.: +91 674 2581636×425; fax: +91 674 2581637.
E-mail address: paridakulamani@yahoo.com (K.M. Parida).
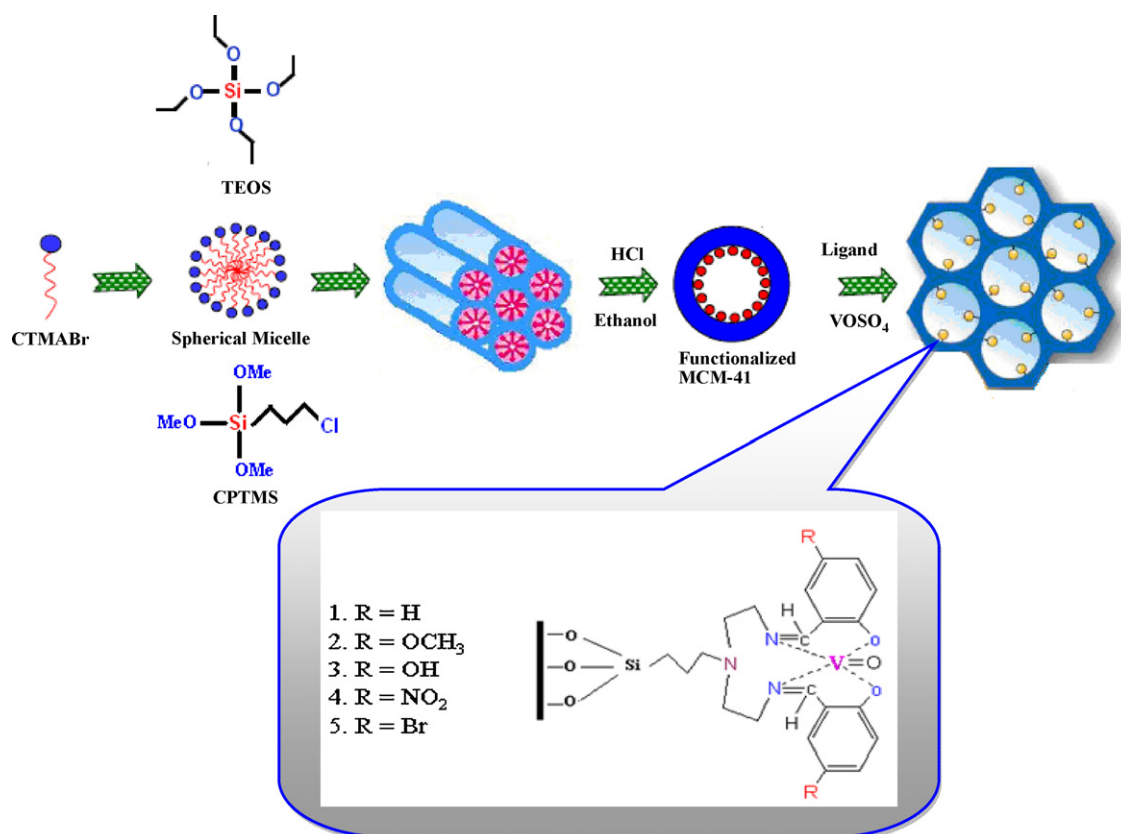
Scheme 1. Schematic representation of the formation of V-MCM-41 within the pore channels of MCM-41.

als is of growing interest [13–15]. In contrast to organic polymers, organic–inorganic hybrid materials do not swell or dissolve in organic solvents. This type of material has many advantages over most organic polymers because of their superior mechanical and thermal stabilities. The surface fuctionalization of mesoporous silica with different organic groups has been reported in literature. Both mesoporous and modified mesoporous silica have already been used for several transition metal catalysts such as manganese, copper, and titanium [16–18]. Obviously, the design of mesoporous silica supported metal complex represents a rapidly growing field that has significantly applied in industry.

Metal complex containing vanadium has been found to be an efficient catalyst for the epoxidation of allylic alcohols but shows relatively poor catalyst for olefin epoxidation. But here in, we are very much delighted to report an efficient vanadium-based catalyst which is found to be effective for the epoxidation of olefins. This catalyst is in tandem with NaHCO$_3$ and aqueous H$_2$O$_2$ in a CH$_3$CN medium at room temperature which display a most pronounced efficiency (% yield, low catalyst loading and high selectivity) in olefin oxidation.

2. Experimental methods

2.1. Materials

(3-Chloropropyl) trimethoxysilane (CPTMS), tetraethyl orthosilicate Si(OC$_2$H$_4$)$_4$ (TEOS), cetyl trimethylammonium-bromide (CTAB), cyclohexene, styrene, norbornene, allylic alcohol, 1-octene, cyclooctene, crotylalcohol, VOSO$_4$·H$_2$O (Aldrich), salicyldehyde, diethylene triamine (CDH), and acetonitrile (Across) were used without further purification.

2.2. Synthesis procedures

2.2.1. Preparation of hybrid mesoporous material: chloro functionalized MCM-41 (CP-MCM-41)

Parent silica MCM-41 was prepared by a standard procedure [19]. Organic modified mesoporous silica with 3-chloropropyltrimethoxysilane(3-CPTMS) (Scheme 1) was prepared according to litreture [20], using C$_{16}$H$_{33}$N(CH$_3$)$_3$Br (CTAB) as templete, tetraethylorthosilicate (TEOS) as silica precurser and 3-CPTMS as organoalkoxysilane precurser. The mixture contained CTAB/TEOS/CPTMS/NaOH/H$_2$O (1.0:8.16:1.05:2.55:4857) based on molar ratio. The mixture of CTAB (2.0 g, 5.49 mmol), 2.0 M of NaOH (aq) (7.0 ml, 14.0 mmol) and H$_2$O (480 g, 26.67 mmol) was heated at 80 °C for 30 min to reach pH 12.3. To this clear solution, TEOS (9.34 g, 44.8 mmol) and CPTMS (1.03 g, 5.75 mmol) were added sequentially and rapidly via injection. Following the injection, a white precipitation was observed after 3 min of stirring. The reaction temperature was maintained at 80 °C for 2 h. The product was isolated by hot filtration, washed with copious amount of water and ethanol and dried under vacuum. To this dried product, an acid extraction process was performed in a methanol (100 ml) mixture of concentrated hydrochloric acid (1.0 ml) at 60 °C for 6 h. with stirring. Resulting surfactant removed product was filtered and washed with water and ethanol and dried under vacuum.

2.2.2. Synthesis of schiffbase ligand

To an ethanolic solution of salicyldehyde (2.12 ml, 20 mmol) a solution of diethylenetriamine (0.96 ml, 10 mmol) was added. The resulting yellow colour solution was allowed to reflux for 2 h. The excess of solvent was removed under vacuum and a dark yellow oily product was obtained. In a simillar manner various substituted ligands were synthesized by taking substituted salicyldehydes.

2.2.3. Synthesis of V-MCM-41

To a suspension of freshly dried CP-MCM-41 (1 g) in 40 ml of ethanol, a solution of 3.1 mmol of above prepared ligand in 10 ml of ethanol was added and the resulting solution was refluxed for 10 h. The whole solution turned yellowish upon addition of ligand. The solid was separated, washed repeatedly with ethanol to remove the unreacted ligand. $VOSO_4$ (1.56 g, 6.2 mmol) was added in 25 ml ethanol to this solid. The solution immediately turned light green indicating immobilization of vanadium, and the final product is abbreviated as V-MCM-41. Atomic absorption spectrometric analysis showed vanadium content in the sample is ca. 0.32%.

2.3. Physico-chemical characterizations

Powder X-ray diffraction (XRD) patterns of the samples were obtained on Rigaku D/Max III VC diffractometer with Cu Kα radiation at 40 kV and 40 mA in the range of $2\theta = 0$–$10°$. The scanning rate was $2°$ min^{-1}. Nitrogen adsorption–desorption isotherms were measured at liquid nitrogen temperature using ASAP 2020 (Micromeritics). Before the measurement, the samples were out gassed at $100°C$ for 3 h to evacuate the physically adsorbed moisture. Specific surface area was calculated using BET method. Solid-state ^{13}C and ^{29}Si cross-polarization magic-angle spinning NMR spectra were recorded at 100.58 and 79.46 MHz, respectively using a Bruker Avance 400 MHz spectrometer.

The FT-IR spectra of the samples were recorded using Varian 800-FT-IR in KBr matrix in the range of 4000–400 cm^{-1}. The coordination environments of the samples were examined by diffuse-reflectance UV–vis spectroscopy. The spectra were recorded in Varian-100 spectrophotometer in the wavelength range of 200–800 nm in $BaSO_4$ phase. The V loading in the catalyst and in the leaching solution was determined by atomic absorption spectroscopy (AAS) with a PerkinElmer Analysis 300 using acetylene (C_2H_2) flame.

2.4. Catalytic reaction

Catalytic test of the prepared heterogeneous catalyst (V-MCM-41) was carried out in a 100 ml two-necked round bottom flask fitted with a reflux condenser. An acetonitrile (10 ml) solution containing a given substrate (10 mmol) and 0.05 g catalyst was taken. To this $NaHCO_3$ (2.5 mmol) and 30% H_2O_2 (30 mmol) were added. Reaction was carried out at room temperature. To get an effective result, an aliquot of the reaction solution was withdrawn from the reaction solution through the help of a syringe. The reaction products were analyzed by off-line gas chromatography (Shimadzu GC-2010) equipped with a capillary column (ZB-1, 30 m length 0.53 mm I.D. and 3.0 μ film thickness) using flame ionization detector (FID). The response factor is calculated by dividing initial mole percent of olefins with initial area percent (olefin peak area from GC). The unreacted moles of cycloalkene remained in the reaction mixture were calculated by multiplying response factor with the area percentage of the GC peak for olefins obtained after the reaction.

The conversion and selectivity were calculated as follows:

$$conversion\,(mol\%) = \left[\frac{initial\,mol\% - final\,mol\%}{initial\,mol\%}\right] \times 100$$

$$epoxide\,selectivity = \frac{GC\,peak\,area\,of\,epoxide}{GC\,peak\,area\,of\,all\,products} \times 100$$

3. Results and discussion

3.1. Characterization of the heterogeneous catalyst

3.1.1. Powder X-ray diffraction

Fig. 1 shows the powder XRD patterns of MCM-41, CP-MCM-41 and V-MCM-41. In case of MCM-41 four diffraction peaks corresponding to Miller indices (1 0 0), (1 1 0), (2 0 0), and (2 1 0) in the range $2\theta = 2$–$8°$ imply that of typical hexagonal structure. However, after organo-functionalization and metal complex loading there is a slight decrease in intensity with broadening of corresponding peaks indicating a slight disorder in the CP-MCM-41 and V-MCM-41. The addition of organic group probably distorts the regular liquid crystalline array of the template and lowers the long-range order of the MCM-41 mesostructure. This is evidenced by the steric effect that becomes more significant when larger or more abundant organic species are added. This is not interpreted as a severe loss of long range ordering of the silica framework [21,22].

3.1.2. N$_2$ sorption studies

N_2 adsorption–desorption isotherms of MCM-41, CP-MCM-41 and V-MCM-41 are given in Fig. 2. Analysis of N_2 adsorption and desorption data exhibit a typical type-IV isotherm (defined by IUPAC) with a small hysteresis for neat MCM-41, CP-MCM-41 and V-MCM-41, characteristic for a mesoporous structure. The relative pressure at which pores are filled is shifted to a lower value for modified samples in comparison to the parent materials, resulting in decrease in BET specific surface area, pore volume and pore diameter. The results are presented in Table 1. The nitrogen sorption study exhibits that the BET surface area of MCM-41 is 1280 m^2 g^{-1} and the mesopore volume is 1.19 cm^3/g. The average pore diametre is calculated to be 30.7 Å using the BJH method. All calculated values are in agreement with those reported for good quality mesoporous silica. CP-MCM-41 shows less N_2 uptake (BET surface area
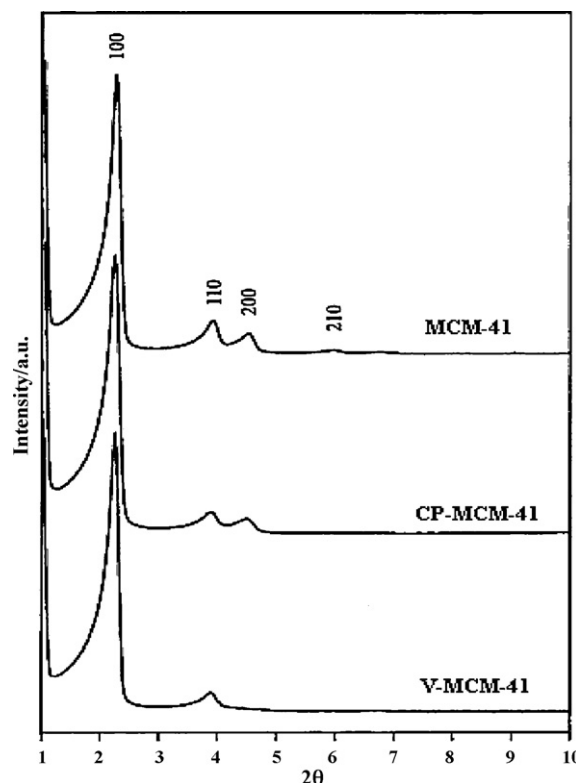

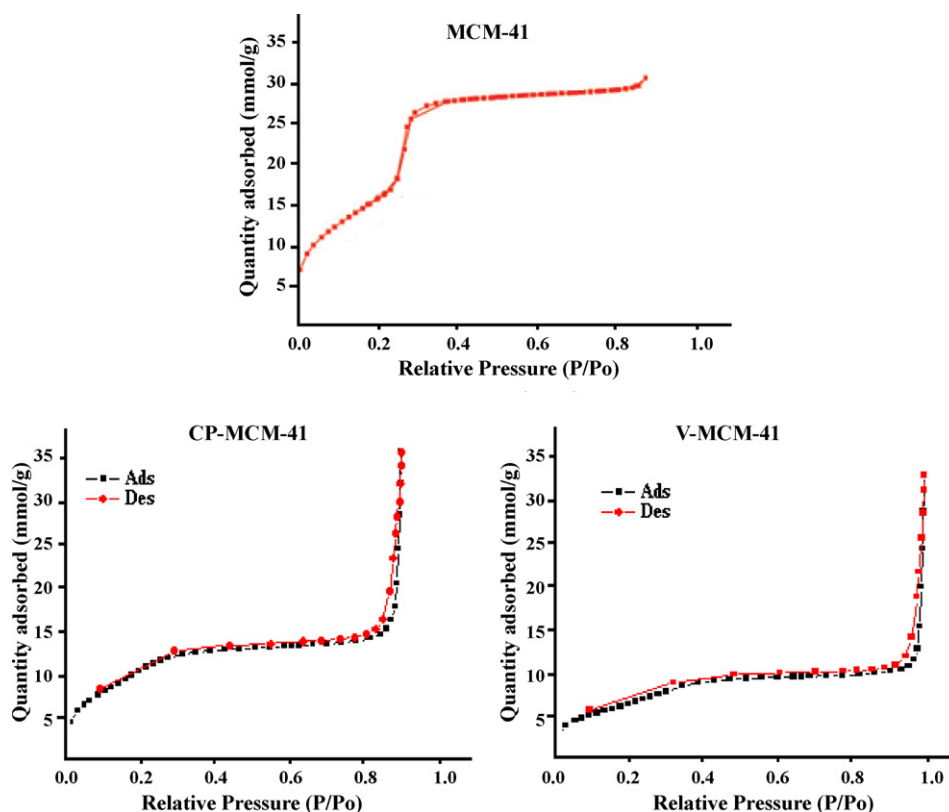**Fig. 1.** XRD spectra of MCM-41, CP-MCM-41, and V-MCM-41.

Fig. 2. N$_2$ adsorption–desorption isotherms of MCM-41, CP-MCM-41, and V-MCM-41.

983 m^2 g^{-1}) and pore volume 1.03 cm^3/g and V-MCM-41 shows further less N$_2$ uptake (BET surface area 584 m^2 g^{-1}) and pore volume 0.68 cm^3/g. We can conclude that complex modified samples possess lower pore volume and pore size distributions compared to its parent materials. With an increase in bulkiness inside the pores, the hysteresis occurred at lower P/P_0 indicating the decrease of pore size. This is a clear indication of immobilization of V complex inside the pore channel of mesoporous silica [23].

3.1.3. ^{13}C CP-MAS NMR studies

The ^{13}C CP-MAS NMR spectrum of CPTMS functionalized MCM-41 is shown in Fig. 3(a). The sharp peak at 10.4 ppm is ascribed to the carbon atom bonded to silicon. The signal at 22.4 ppm corresponds to methylene carbon and the peak around at 50 ppm can be attributed to carbon atom attached to the chlorine atom. In case of CP-MCM-41 one can observe three distinct peaks for thee different carbon atoms. Three similar types of peaks are also observed for V-MCM-41 in the range of 0–40 ppm. This may be due to partial change in the environment after the replacement of chlorine by nitrogen. The ^{13}C CP-MAS NMR spectra of complex immobilized MCM-41(3(b)) show peaks corresponding to aliphatic and aromatic carbons of the schiffbase. Similar resonance shift are observed for all functional group modified schiffbase complex in Fig. 3(c–f).

Table 1
Textural properties of parent MCM-41 and modified mesoporous samples from N$_2$ isotherms at 77 K.

| Samples	BET surface area (m^2 g^{-1})	Pore volume (cm^3 g^{-1})	Pore diameter (Å)
MCM-41	1280	1.19	30.7
CP-MCM-41	983	1.03	26.1
V-MCM-41	584	0.68	20.6

3.1.4. ^{29}Si CP-MAS NMR studies

The degree of functionalization, i.e. the covalent linkage between the silanol groups and the organic moiety on the mesostructured materials can be monitored by means of ^{29}Si CP-MAS NMR spectroscopy. The spectrum of MCM-41 [Fig. 3(g)] generally exhibits three resonance peak at δ −110, −101, and −92 corresponds to Q^4 [siloxane, (SiO)$_4$Si], Q^3 [single silanol,(SiO)$_3$Si(OH)] and Q^2 [geminal silanol,(SiO)$_2$Si(OH)$_2$] sites of the silica framework, respectively. Covalent binding makes the Q^2 signal disappear, decrease Q^3 and concomitantly increase the Q^4 intensity, which is due to consumption of isolated Si—OH and geminal silandiols during condensation process. Two resonance peaks due to the Si environments of Q^4 (δ = −110 ppm) and Q^3 (δ = −102 ppm) can be seen in the organic group modified silica. In addition to these two peaks, the sample displays two more resonance peaks at δ = −68 ppm, assigned to T^3 [C—Si(OSi)$_3$], and at −57 ppm, attributed to T^2 [C—Si(OSi)$_2$(OH)], respectively. The existence T^3 confirms that MCM-41 has been modified by organic moieties [24,25]. The appearance of Q^3 signal indicates the presence of some residual non-condensed OH groups attached to the silicon atom. The ^{29}Si CP-MAS NMR provides direct evidence that the hybrid CP-MCM-41 sample consists of a highly condensed siloxane network with organic group covalently bonded to the mesoporous silica. These two peaks due to the Si atoms of different environments in the organosilane CP-MCM-41 also revealed that both synthesis process and surfactant-extraction treatment did not cause cleavage of the Si—C bonds.
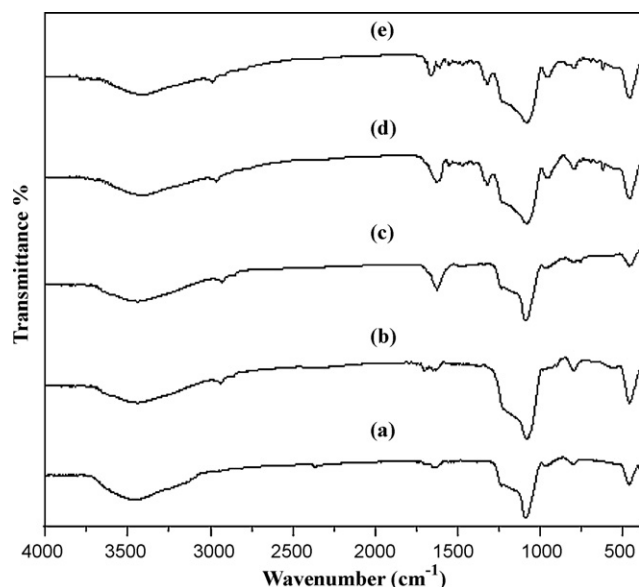
3.1.5. FT-IR studies

To establish the immobilization of vanadium complex inside the pore of organically modified mesoporous silica is a difficult task. However, in our experiment we have developed that IR has been shown to be a powerful characterization in monitoring multistep-assembly of the complex inside the mesoporous silica. Fig. 4 shows
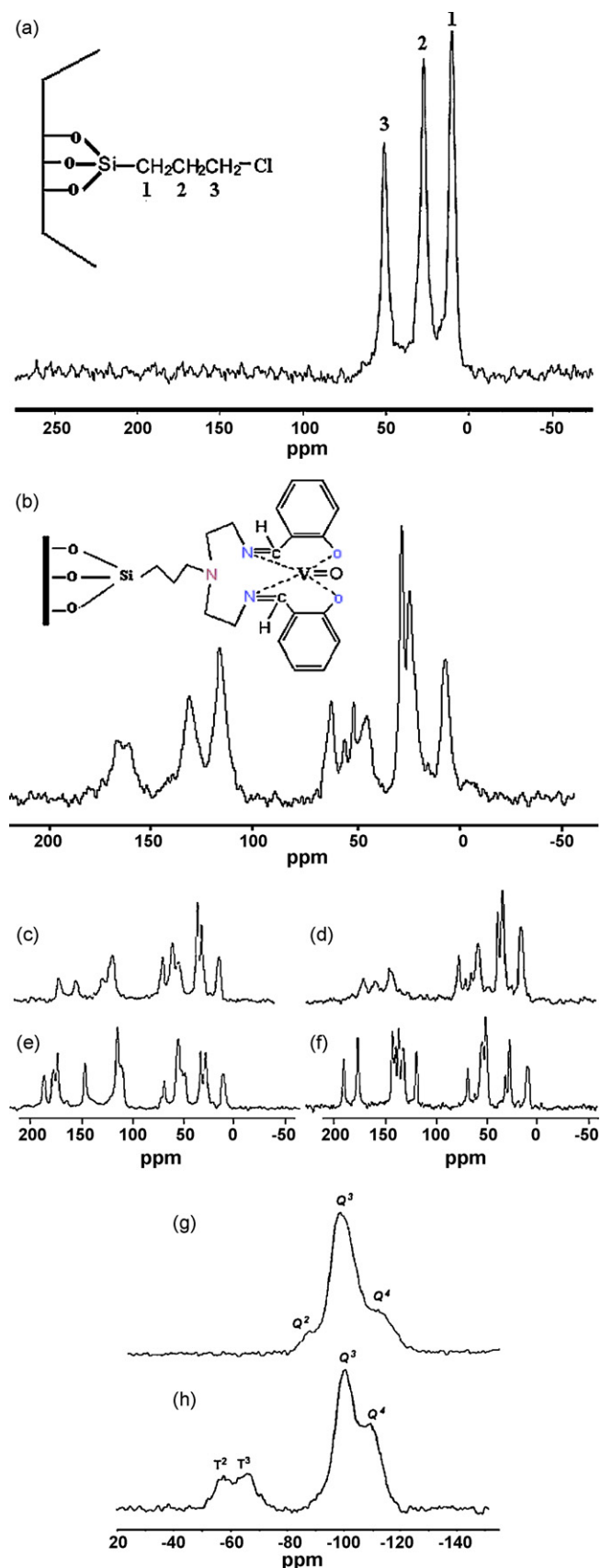
Fig. 4. FT-IR spectra of (a) MCM-41, (b) CP-MCM-41, (c) schiffbase ligand modified CP-MCM-41, (d) V-MCM-41, and (e) V-MCM-41 after recycled.
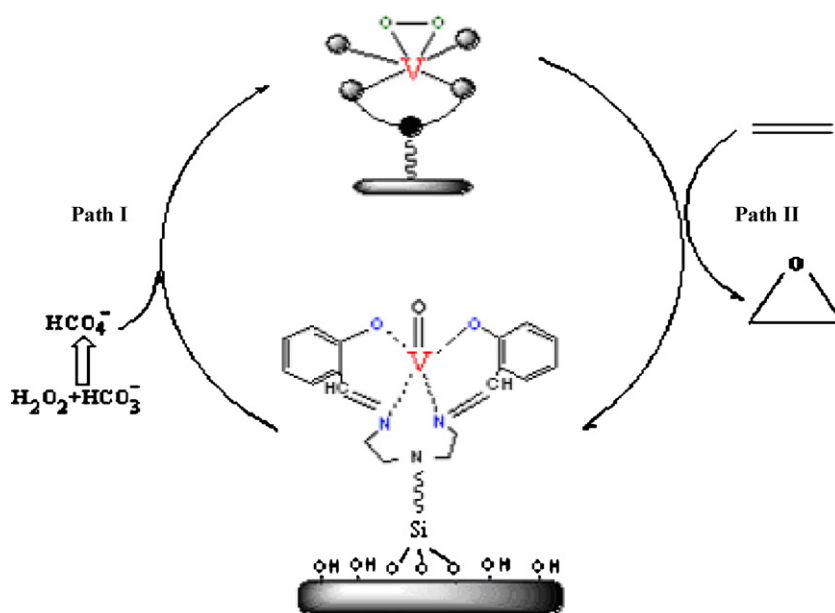
the FT-IR spectra of (a) MCM-41, (b) CP-MCM-41, (c) schiffbase ligand modified CP-MCM-41, (d) V-MCM-41, (e) V-MCM-41 after recycled. The stretching vibration due to Si—O—Si bond of parent MCM-41 as well as in all modified samples appeared around $1050\,cm^{-1}$ indicating that silica framework was not affected, which is in accordance with the XRD result. A peak observed at $780\,cm^{-1}$ is likely to be from the $SiOCH_2CH_2CH_2$— group due to incomplete hydrolysis of TEOS. Generally a weak band within ~2900 appears in case of organic group modified mesoporous silica due to C—H stretching vibration. Upon functionalization with CPTMS a band appeared around $2900\,cm^{-1}$ due to asymmetric stretching vibration of C—H bond in CH_2 unit. In Fig 4(c) a band at $1640\,cm^{-1}$ is due to characteristic of C=N stretching in the ligand modified organic–inorganic hybrid material. The intensity of that particular bond decreased after metal loading and slightly shifted to lower frequency due to coordination with vanadium. Again a band appeared around $970\,cm^{-1}$ due to stretching vibration of V=O [26]. All these data give a clear indication for the attachment of the metal complex to the organic group modified MCM-41. In Fig 4(e), the stretching vibrations do not change significantly, suggesting existence of all the properties in the recycled catalyst.

3.1.6. UV–vis spectral studies

The UV–vis diffuse-reflectance spectra of vanadium schiffbase anchored CP-MCM-41 are added in Fig. 5. It can be seen that a series of characteristic bands of the schiffbase ligand immobilized MCM-41 at 220, 260, 340 and 380 nm emerges in the spectra. The bands can be attributed to a typical electronic transition of the aromatic ring and —C=N— conjugated system in the schiffbase molecule. A broad band is noticed at about 410 nm resulting from the $\pi-\pi^*$ electronic transition of the schiffbase. In case of V-MCM-41 an additional broad band around 580 nm arises due to d–d electronic transition of vanadium present in the complex. Similar types of peaks are also exhibited in case of vanadium–schiffbase complex. Appearance of all types of transition bands in the recycled catalyst indicates the retention of all the properties.
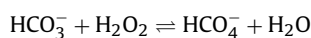
3.2. Catalytic epoxidation reaction

Control experiments were carried out using only H_2O_2 as oxidant, but failed to produce the desired yield. Though H_2O_2 is an

Fig. 3. ^{13}C CP-MAS NMR spectrum of (a) CP-MCM-41, (b) V-MCM-41, (c–f) different functional group attach to ligand in V-MCM-41, ^{29}Si CP-MAS NMR spectrum of (g) MCM-41, and (h) CP-MCM-41

Scheme 2. The possible reaction pathway comprising of path I and path II.

environmentally benign oxidant, but a disadvantage is that high activation energy is required for the oxidation of many organic compounds by using this oxidant. In contrast, the number of organic, non-metal compounds capable of activating H_2O_2 for epoxidation is limited [27]. Again, catalytic efficiency of H_2O_2 when it is used as sole oxidant is rather poor as compared to tert-butylhydroperoxide and peracids in epoxidation reaction. This is due to the poor leaving tendency of the hydroxide ion. However, higher conversion and epoxide selectivity can be achieved by adding a small amount of $NaHCO_3$ to the reaction medium. The addition of $NaHCO_3$ enhances the catalytic activity to many folds due to the formation of peroxomonocarbonate species. A method for activating hydrogen peroxide with bicarbonate was described by Drago et al. [28]. Production of active peroxomonocarbonate ion, HCO_4^- and its involvement in the reaction plays an important role. The formation of HCO_4^- is an equilibrium process and it takes only few minutes. Though vanadium (V) is found to be a relatively poor catalyst for alkene epoxidation, the generation of peroxomonocarbonate in this reaction medium totally changes the reaction scenario. The mechanistic pathway is shown diagrammatically in Scheme 2. The catalytic oxo–peroxo intermediate is formed by the treatment of the HCO_4^- with the complex immobilized MCM-41 (path I). Such a peroxo complex than oxidized olefin (Path II) and itself revert back to oxo complex, which again react with $H_2O_2/NaHCO_3$ to regain its catalytic properties and so on. As peroxomonocarbonate is a more reactive nucleophile compared to H_2O_2 that accelerates the reaction leading to epoxidation.
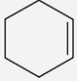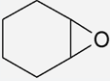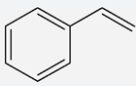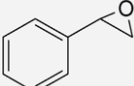
$$HCO_3^- + H_2O_2 \rightleftharpoons HCO_4^- + H_2O$$
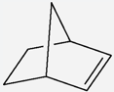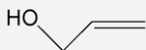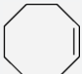
By using 0.25 M of $NaHCO_3$ we got maximum conversion. Increase in concentration of bicarbonate increased the pH of the reaction medium greater than 8, which would reduce the efficiency towards epoxidation reaction. The catalytic epoxidation of various olefins is summarized 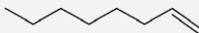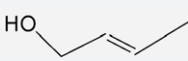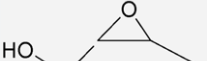in Table 2. Though the correlative literatures shows catalytic activity sequence as cyclooctene > cyclohexene > styrene > 1-octene, opposite to our observations (1-octane > cyclohexene > styrene > cyclooctene). This may presumably be due to easy approach of active species (oxidant) to 1-octene compared to cyclooctene which has a stained ring [29]. However there is marginally change in the yields between 1-octene and cyclooctene. We have also carried out the reaction by using H_2O_2–$NaHCO_3$ in absence of V-MCM-41, but it showed negligible conversion (2%). If the stirring is continued for a longer period of time, conversion rate gradually decreases perhaps due to formation of diols. The ligand structure also influences the relative rates of catalyst towards epoxidation reaction of different olefins [30]. A characteristic epoxidation reactivity profile can be measured for each substitution under identical condition. Substituted aromatic rings with various electron donating (−OMe, −OH) and withdrawing groups such as (–Br, –NO$_2$) have been used in the ligand design and catalytic epoxidation. We found practically no influence of the substitution on the conversion as well as selectivity. These data demonstrate the beneficial influence of designing a complex with sufficiently large flexibility to allow the substrate–complex adduct to adopt a spatial disposition similar to that in the homogeneous phase. A ball-stick model representation of vanadium–schiffbase complex is depicted in Fig. 6.

The epoxidation reaction is markedly influenced by reaction temperature. High yield of epoxide products were obtained at room temperature especially for olefinic alcohol, i.e. for allylic alcohol and cinnamyl alcohol. Olefin group is chemoselectively oxidized
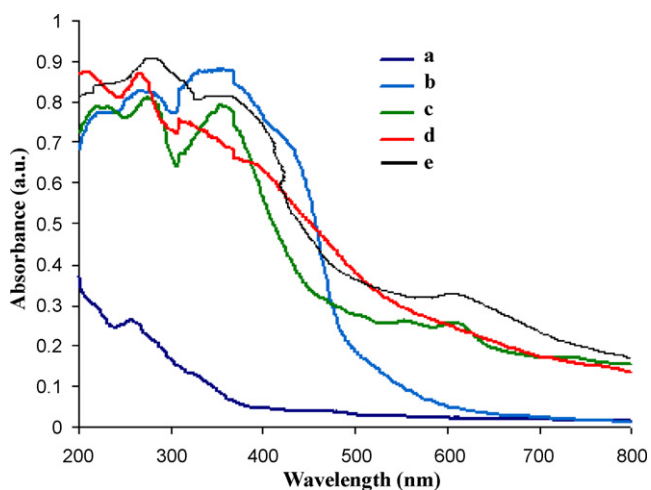

Fig. 5. UV–vis spectra of (a) CP-MCM-41, (b) schiffbase ligand modified CP-MCM-41, (c) V-MCM-41, (d) V-MCM-41 after recycled, and (e) vanadium–schiffbase complex.

Table 2
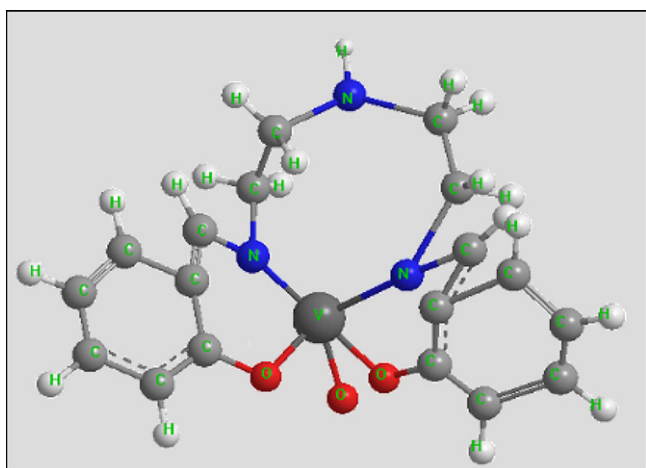Details of the catalytic epoxidation of olefinic compounds.

Entry	Substrate	Product	Time (h)	Conversion (%)	Selectivity	
					Epoxide	Others
1	(cyclohexene)	(cyclohexene oxide)	8	84	94	6
2	(styrene)	(styrene oxide)	8	83	93	7
3	(norbornene)	(norbornene oxide)	8	87	97	3
4	HO— (allyl alcohol)	HO— (glycidol)	6	95	94	6
5	(cyclooctene)	(cyclooctene oxide)	8	82	98	2
6	(1-octene)	(1,2-epoxyoctane)	8	88	90	10
7	HO— (crotyl alcohol)	HO— (epoxide)	6	90	94	6

Reaction conditions: substrate 10 mmol, amount of catalyst 0.05 g, acetonitrile 10 ml, 2.5 mmol $NaHCO_3$, 30 mmol H_2O_2, reaction occurred at room temperature.

to epoxide, alcohol groups remain unchanged. We employed the epoxidation reaction of olefins at various temperatures in order to check the exact effect of temperature on the reaction. Chemoselectivity for olefinic alcohols is presumed to be lost as some undesired product formation takes place at higher temperature. Besides epoxide, epoxy aldehyde is also formed to some extent. It is the alcoholic group in the olefinic alcohol, which is activated at higher temperature, i.e. around 70–80 °C. Also at higher temperature a part of $NaHCO_3$ is converted to Na_2CO_3, which will increase the pH of the reaction and facilitates the higher decomposition of H_2O_2 [29].

$$2NaHCO_3 \rightarrow Na_2CO_3 + CO_2 + H_2O$$
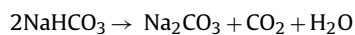
This will lead to reduce the yield by deactivating the reaction. Several attempts were also made to effect the epoxidation reaction in a biphasic solvent system. We have performed the reaction with methylbenzene, dichloromethane, diethyl ether, ethyl acetate, or pentane with acetonitrile in equimolar proportion which produced no significant result. Presumably they may suppress the formation of HCO_4^- which decreases the promotional effect.

In addition, the stability of the modified materials was studied by recycling the recovered catalyst. At the end of the reaction, the solid catalyst was separated from the reaction solution, thoroughly washed with ethanol, dried at room temperature and reused under similar reaction conditions. The reused catalyst showed a slight lower catalytic activity in successive runs. These trends can be interpreted by considering the leaching process, as it is more important due to economic point of view. Probably, in fact leaching is a particular problem for heterogeneous catalyst in liquid phase reaction. To test if vanadium is leaching out of the catalyst, the reaction mixture was filtered out after the reaction and was subjected to atomic absorption spectroscopic analysis. The analysis showed the absence of vanadium in the filtrate. Besides that the filtrate mixture also did not show any catalytic activity towards epoxidation reaction. These results indicate that the catalyst is regenerable and reusable which has the advantage over the homogeneous counterpart.

4. Conclusions

Covalent functionalization of vanadium–schiffbase complex onto the CP-MCM-41 was successfully achieved by a multiple synthetic procedure. The presence of d (100) in the XRD pattern confirmed the retention of hexagonal ordering even after functionalization and metal complex loading. The effect of vanadium–schiffbase complex loading on the physical properties of MCM-41 (surface area and pore parameters) was explored by nitrogen sorption. The progressive change with different modifications on Type IV isotherm confirms that the immobilization

Fig. 6. Model representation of vanadium–schiffbase complex.

of vanadium–schiffbase complex causes pore narrowing, which resulted in decrease in the mesoporosity of MCM-41. This is also supported by a decrease in surface area, pore volume and pore diameter of MCM-41. The ^{13}C CP-MAS NMR spectra of the complex immobilized sample shows all possible peaks corresponding to both the aliphatic and aromatic carbon atoms. Solid-state ^{29}Si CP-MAS NMR showed that the organic group is successfully bonded to mesoporous silica. FT-IR and diffuse-reflectance UV–vis spectra confirmed the immobilization and retention of the surface properties of the catalyst after the catalytic reaction. The most interesting features of the present work is the revealing of chemistry that display a most pronounced efficiency with NaHCO$_3$ as co-catalyst and H$_2$O$_2$ as oxidant in a CH$_3$CN medium at room temperature. The reaction suggests that nature of the catalyst and reaction medium can influence the reaction. This method is green and economical from environmental point of view. Repeated recycled study without loss of activity shows the stability of V-MCM-41.

Acknowledgements

References

[1] B.S. Lane, K. Burgess, Chem. Rev. 103 (2003) 2457–2474.
[2] T. Katsuki, K.B. Sharpless, J. Am. Chem. Soc. 113 (1991) 7063–7064.
[3] R. Noyori, M. Aoki, K. Sato, Chem. Commun. (2003) 1986–1997.
[4] M.K. Tse, M. Klawonn, S. Bhor, C. Do1bler, G. Anilkumar, H. Hugl, W. Ma1gerlein, M. Beller, Org. Lett. 7 (2005) 987–990.
[5] E.S. Gould, R.R. Hiatt, K.C. Irwin, J. Am. Chem. Soc. 90 (1968) 4573–4579.
[6] B. Jarrais, C. Pereira, A.R. Silva, A.P. Carvalho, J. Pires, C. Freire, Polyhedron 28 (2009) 994–1000.
[7] S.I. Mostafa, S. Ikeda, B. Ohtani, J. Mol. Catal. A 225 (2005) 181–188.
[8] G. Yin, M. Buchalova, A.M. Danby, C.M. Perkins, D. Kitko, J.D. Carter, W.M. Scheper, D.H. Busch, Inorg. Chem. 45 (2006) 3467–3474.
[9] W. Zhang, J.L. Loebach, S.R. Wilson, E.N. Jacobsen, J. Am. Chem. Soc. 112 (1990) 2801–2803.
[10] Q.-H. Fan, Y.-M. Li, A.S.C. Chan, Chem. Rev. 102 (2002) 3385–3466.
[11] C.T. Kresge, M.E. Leonowicz, W.J. Roth, J.C. Vartuli, J.S. Beck, Nature 359 (1992) 710–712.
[12] D.Y. Zhao, J.L. Feng, Q.S. Huo, N. Melosh, G.H. Fredrickson, B.F. Chmelka, G.D. Stucky, Science 279 (1998) 548–552.
[13] A. Stein, B.J. Melde, R.C. Schroden, Adv. Mater. 12 (2000) 1403.
[14] S.-J. Bae, S.-W. Kim, T. Hyeon, B.-M. Kim, Chem. Commun. (2000) 31–32.
[15] D.D. Das, A. Sayari, Stud. Surf. Sci. Catal. 170 (2007) 1197–1204.
[16] D.E. de Vos, I.F.J. Vankelecom, P.A. Jacobs (Eds.), Chiral Catalyst Immobilisation and Recycling, Wiley–VCH Verlag, Weinheim, 2000, p. p19.
[17] D.E. de Vos, M. Dams, B.F. Sels, P.A. Jacobs, Chem. Rev. 102 (2002) 3615–3640.
[18] Q.-H. Xia, H.-Q. Ge, C.-P. Ye, Z.-M. Liu, K.-X. Su, Chem. Rev. 105 (2005) 1603–1662.
[19] D. Brunel, Micropor. Mesopor. Mater. 27 (1999) 329–344.
[20] S. Huh, J.W. Wiench, J. Yoo, M. Pruski, W.S.-Y. Lin, Chem. Mater. 15 (2003) 4247.
[21] M. Kruk, M. Jaroniec, Y. Sakamoto, O. Terasaki, R. Ryoo, C.H. Ko, J. Phys. Chem. 104B (2000) 292–298.
[22] W. Hammond, E. Prouzet, S.D. Mohanti, T.J. Pinnaviam, Micropor. Mesopor. Mater. 27 (1999) 19–25.
[23] H. Yang, G. Zhang, X. Hong, Y. Zhan, J. Mol. Catal. A: Chem. 210 (2004) 143–148.
[24] D. Jiang, Q. Yang, H. Wang, H. Chen, G. Zhu, J. Yang, C. Li, J. Catal. 239 (2006) 23–29.
[25] D. Jiang, Q. Yang, J. Yang, L. Zhang, G. Zhu, C. Li, Chem. Mater. 17 (2005) 6154–6160.
[26] R.A. Shiel, K. Venkatasubbaiah, C.W. Jones, Adv. Synth. Catal. 350 (2008) 2823–2834.
[27] W. Adam, C.R. Saha-Moller, P.A. Ganeshpure, Chem. Rev. 01 (2001) 3499–3548.
[28] R.S. Drago, K.M. Frank, Y.-C. Yang, G.W. Wagner, Proceedings of 1997 ERDEC Scientific Conference on Chemical and Biological Defense Research, ERDEC, 1998.
[29] S.K. Maiti, S. Dinda, N. Gharah, R. Bhattacharyya, New J. Chem. 30 (2006) 479–489.
[30] A. Murphy, A. Pace, T.D.P. Stack, Org. Lett. 6 (2004) 3119–3122.